

Active Control and Spatial Mapping of Mid-Infrared Propagating Surface Plasmons

T. Ribaldo,¹ E. A. Shaner,² S. S. Howard,³ C. Gmachl,³ X. J. Wang,⁴ F.-S. Choa,⁵ and D. Wasserman^{1,*}

¹Department of Physics, University of Massachusetts Lowell, One University Avenue, Lowell, MA, 01854, USA

²Sandia National Labs, P.O. Box 5800, Albuquerque, NM 87185

³Department of Electrical Engineering, Princeton University Princeton, NJ 08544

⁴Adtech Optics Inc., City of Industry, CA 91748

⁵Dept. of CSEE, University of Maryland Baltimore County, Baltimore, MD 21250

*Corresponding author: daniel.wasserman@uml.edu

Abstract: Periodic arrays of subwavelength apertures in metal films have been shown to exhibit strongly enhanced transmission at wavelengths determined by the periodicity of the film as well as the optical properties of the metal and surrounding dielectric material. Here we investigate the coupling between such a grating and a Quantum Cascade Laser. By actively tuning the optical properties of our grating, we control the coupling of laser light to the plasmonic structure, switching our grating from a predominantly transmitting state to a state that allows coupling to propagating surface waves, which can then be imaged on the metallic surface.

©2009 Optical Society of America

OCIS codes: (240.6680) Surface plasmons; (250.5403) Plasmonics

References and links

1. D. Heitmann and H. Raether, "Light emission of nonradiative surface plasmons from sinusoidally modulated silver surfaces," *Surf. Sci* **59**, 17-22 (1976).
2. R. H. Ritchie, E. T. Arakawa, J. J. Cowan, and R. N. Hamm, "Surface-Plasmon Resonance Effect in Grating Diffraction," *Phys. Rev. Lett.* **21**, 1530-1533 (1968).
3. T. W. Ebbesen, H. J. Lezec, H. F. Ghaemi, T. Thio, and P. A. Wolff, "Extraordinary optical transmission through sub-wavelength hole arrays," *Nature* **391**, 667-669 (1998).
4. F. García-Vidal, L. Martín-Moreno, H. J. Lezec and T. W. Ebbesen, "Focusing light with a single subwavelength aperture flanked by surface corrugations," *Appl. Phys. Lett.* **83**, 4500-4502 (2003).
5. C. Genet, T. W. Ebbesen, "Light in Tiny Holes," *Nature* **445**, 39-46 (2007).
6. K. R. Rodriguez, S. Shah, S. M. Williams, S. Teeters-Kennedy, and J. V. Coe, "Enhanced infrared absorption spectra of self-assembled alkanethiol monolayers using the extraordinary infrared transmission of metallic arrays of subwavelength apertures," *J. Chem. Phys.* **21**, 8671-8675 (2004).
7. L. Martín-Moreno, F. J. García-Vidal, H. J. Lezec, A. Degiron, and T. W. Ebbesen, "Theory of Highly Directional Emission from a Single Subwavelength Aperture Surrounded by Surface Corrugations," *Phys. Rev. Lett.* **90**, 167401 (2003).
8. H. Ditlbacher, J. R. Krenn, G. Schider, A. Leitner, and F. R. Aussenegg, "Two-dimensional optics with surface plasmon polaritons," *Appl. Phys. Lett.* **81**, 1762-1764 (2002).
9. L. Martín-Moreno, F. J. García-Vidal, H. J. Lezec, K. M. Pellerin, T. Thio, J. B. Pendry, and T. W. Ebbesen, "A theory of extraordinary optical transmission through subwavelength hole arrays," *Phys. Rev. Lett.* **86**, 1114-1117 (2001).
10. R. Müller, V. Malyarchuk, and C. Lienau "Three-dimensional theory on light-induced near-field dynamics in a metal film with a periodic array of nanoholes," *Phys. Rev. B* **68**, 205415-205423 (2003).
11. S.-H. Chang, S. Gray, and G. Schatz, "Surface plasmon generation and light transmission by isolated nanoholes and arrays of nanoholes in thin metal films," *Opt. Express* **13**, 3150-3165 (2005).
12. P. D. Flammer, I. C. Schick, R. T. Collins, and R. E. Hollingsworth, "Interference and resonant cavity effects explain enhanced transmission through subwavelength apertures in thin metal films," *Opt. Express* **15**, 7984-7993 (2007).
13. H. Lezec and T. Thio, "Diffracted evanescent wave model for enhanced and suppressed optical transmission through subwavelength hole arrays," *Opt. Express* **12**, 36293651 (2004).
14. P. Lalanne and J. Hugonin, "Interaction between optical nano-objects at metallo-dielectric interfaces," *Nat. Phys.* **2**, 551-556 (2006).

15. J. B. Pendry, L. Martín-Moreno, and F. J. Garcia-Vidal, "Mimicking Surface Plasmons with Structured Surfaces," *Science* **305**, 847-848 (2005).
16. F. García de Abajo and J. J. Sáens, "Electromagnetic Surface Modes in Structured Perfect-Conductor Surfaces," *Phys. Rev. Lett.* **95**, 233901 (2005).
17. H. Liu and P. Lalanne, "Microscopic Theory of Extraordinary transmission," *Nature* **452** 728-731 (2008).
18. D. Pacifici, H. J. Lezec, R. J. Walters, and H. A. Atwater, "Universal optical transmission features in periodic and quasiperiodic hole arrays," *Opt. Express* **16** 9222-9238 (2008).
19. T. Ribauto, B. Passmore, K. Freitas, E. A. Shaner, J. G. Cederberg, and D. Wasserman, "Loss mechanisms in mid-infrared extraordinary optical transmission gratings," *Opt. Express* **17**, 666-675 (2009).
20. H. F. Ghaemi, T. Thio, D. E. Grupp, T. W. Ebbesen, and H. J. Lezec, "Surface plasmons enhance optical transmission through subwavelength holes," *Phys. Rev. B* **58**, 6779-6782 (1998).
21. E. A. Shaner, J. Cederberg, and D. Wasserman, "Current-tunable mid-infrared extraordinary transmission gratings," *Appl. Phys. Lett.* **91**, 181110 (2007).
22. G. Gagnon, N. Lahoud, G. A. Mattiussi, and P. Berini, "Thermally Activated Variable Attenuation of Long-Range Surface Plasmon-Polariton Waves," *J. Lightwave Technol.* **24**, 43914402 (4391).
23. D. Pacifici, H. J. Lezec, and H. A. Atwater, "All-optical modulation by plasmonic excitation of CdSe quantum dots," *Nat. Photonics* **1**, 402-406 (2007).
24. J. Gómez Rivas, P. Haring Bolivar, and H. Kurz, "Thermal switching of the enhanced transmission of terahertz radiation through subwavelength apertures," *Opt. Lett.* **29**, 16801682 (2004).
25. C. Janke, J. Gómez Rivas, P. Haring Bolivar, and H. Kurz, "All-optical switching of the transmission of electromagnetic radiation through subwavelength apertures," *Opt. Lett.* **30**, 2357-2359 (2005).
26. J. Gómez Rivas, M. Kuttge, H. Kurz P. Haring Bolivar and J. A. Sánchez-Gil, "Low-frequency active surface plasmon optics on semiconductors," *Appl. Phys. Lett.* **88**, 082106 (2006).
27. E. Hendry, F. J. Garcia-Vidal, L. Martín-Moreno, J. Gómez Rivas, M. Bonn, A. P. Hibbins, and M. J. Lockyear, "Optical Control over Surface-Plasmon-Polariton-Assisted THz Transmission through a Slit Aperture," *Phys. Rev. Lett.* **100**, 123901 (2008).
28. J. S. Blakemore, "Semiconducting and other major properties of gallium arsenide," *J. Appl. Phys.* **53**, R123-R181 (1982).
29. C. P. Christensen, R. Joiner, S. T. K. Nieh, and W. H. Steier, "Investigation of infrared loss mechanisms in high-resistivity GaAs," *J. Appl. Phys.* **45**, 4957-4960 (1974).
30. W. L. Barnes, "Surface plasmon-polariton length scales: a route to sub-wavelength optics," *J. Opt. A: Pure Appl. Opt.* **8**, S87-S93 (2006).
31. M. A. Ordal, L. L. Long, R. J. Bell, S. E. Bell, R. R. Bell, R. W. Alexander, Jr., and C. A. Ward, "Optical properties of the metals Al, Co, Cu, Au, Fe, Pb, Ni, Pd, Pt, Ag, Ti, and W in the infrared and far infrared," *Appl. Opt.* **22**, 1099-1119 (1983).

The optical properties associated with subwavelength corrugations [1,2], apertures [3] or slits [4] in metallic films have received significant attention, not only for fundamental scientific investigations, but for applications in display [5], sensing [6], beam steering [7], and on-chip communication or interconnect technologies [8]. For periodic arrays of subwavelength apertures, resonant transmission at wavelengths larger than an individual aperture diameter is observed, a phenomenon labeled Extraordinary Optical Transmission (EOT) [3]. For a broad range of wavelengths, the coupling of incident radiation to such structures involves the excitation of surface plasmon polaritons (SPPs) at the metal/dielectric interfaces.

The SPP can be thought of as a collective charge oscillation coupled to electromagnetic propagating waves. The dispersion relation for these excitations can be found by solving Maxwell's Equations for surface propagating waves, using the appropriate boundary conditions. The resulting expression gives the SPP wavevector k_{spp} as a function of the excitation frequency (Eq. (1a)), where ϵ_d and ϵ_m are the relative permittivities of the dielectric material and the metal, respectively.

$$(a) \quad k_{spp}^2 = \frac{\omega^2}{c^2} \left(\frac{\epsilon_d \epsilon_m}{\epsilon_d + \epsilon_m} \right) \quad (b) \quad k_{spp} = k_{xph} \pm \frac{2\pi}{a_o} m, \quad k_{xph} = k_{ph} \sin \theta \quad (1)$$

In order to couple a free space photon into such a mode, momentum must be conserved. For periodically modulated metal films, this is achieved by means of a grating wavevector associated with the periodicity of the film. The resulting expression, for a SPP propagating in the x-direction only, can be written as shown in Eq. (1b), where a_o is the periodicity of the metal film, m is an integer, and k_{xph} is the in-plane momentum component of the total photon momentum k_{ph} , for a photon incident upon a plasmonic surface at an angle θ [2].

The past decade has seen numerous investigations of the EOT phenomenon, with most arguing for the SPP as the primary enhanced transmission mechanism [9-14], at least for non-perfectly conducting metals [15]. Early analytical studies investigated the EOT phenomenon from a macroscopic mode-expansion approach [9,16], while more recently, multiple groups have demonstrated microscopic theories for the EOT phenomenon based on the scattering of excited surface waves from the array of subwavelength apertures, and the interaction of the scattered waves with light directly transmitted through the apertures [17,18].

Here we investigate the transmission of coherent mid-infrared (mid-IR) radiation through an EOT structure. The study of transmission through EOT structures typically relies on the macroscopic response of the grating to incident radiation (measuring transmitted, reflected, or diffracted light intensity) [19]. However, such experiments cannot differentiate between directly transmitted light, and light which couples to surface modes and is then re-radiated. By use of a novel spectral and spatial characterization set-up, we are able to measure not only direct transmission as a function of wavelength, but also the coupling of the incident radiation to propagating surface modes on our metal/dielectric interface.

In order to investigate the transmission through, and surface mode propagation on, mid-IR EOT gratings, the direction of expected propagation must be determined. At normal incidence, for light polarized in the x-direction, the forward (1,0) and backward (-1,0) propagating modes are degenerate. However, for $\theta \neq 0$, these two SPP modes split, which is typically evidenced by a splitting of the primary peak in the grating transmission spectra [20]. Thus, photons resonant with the lower frequency ν_- peak should couple to SPPs propagating in the -x direction, while those resonant with the higher frequency ν_+ transmission peak would be expected to couple to SPPs propagating in the +x direction.

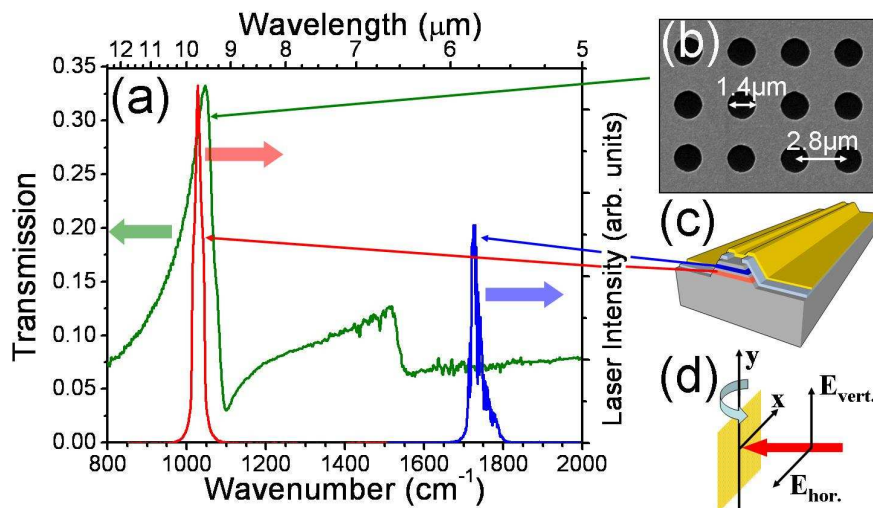


Fig. 1. (a). QCL emission spectrum (short wavelength-blue, long wavelength-red) and normal incidence, room temperature (RT) broadband transmission through EOT grating sample (green). (b) Schematic of dual wavelength QCL, (c) Scanning Electron Micrograph of EOT grating surface, and (d) diagram of coordinate system used in this work.

For on-chip interconnect or sensing applications, directional control of a propagating surface excitation would be highly desirable. This could be achieved by switching between light of frequencies ν_- and ν_+ to couple to modes propagating in the -x and +x directions, respectively. Alternatively, if one could spectrally shift the optical properties of the plasmonic structure itself, monochromatic light incident upon a metal/dielectric interface could be directed in opposite directions simply by tuning the plasmonic structure. Recently, active control of a plasmonic structure has been proposed and achieved [21-23], suggesting that such directional control of SPPs is feasible. Much of the work on tunable plasmonic materials has focused on the THz frequency range [24-27], with relatively little effort, thus far, in the mid-IR spectral range, despite the mid-IR's importance for sensing and beam-

steering applications. In addition, the long SPP propagation lengths in the mid-IR (100's of μm), makes possible the use of far-field techniques to image the propagating surface waves. This allows for a clear demonstration of controlled coupling to waves on our active plasmonic surface, and may also aid in the understanding of the mid-IR EOT process.

The plasmonic structure studied in this work is an EOT grating with its primary peak ($m=1$, in Eq. (1b)) transmission at 1053 cm^{-1} ($\sim 9.5\text{ }\mu\text{m}$). The grating consists of a thin Ti/Au (10nm/60nm) film with $1.4\text{ }\mu\text{m}$ diameter apertures in a square lattice pattern with periodicity of $2.8\text{ }\mu\text{m}$ (Fig. 1(b)), deposited upon a semi-insulating GaAs wafer. Broadband spectral characterization of the EOT grating (Fig. 1(a)) was performed using a Bruker V70 Fourier Transform Infrared (FTIR) spectrometer. Normal incidence transmission for this structure demonstrates a transmission of 33% at the primary EOT peak (metal covers all but 21% of the sample surface, indicating that we are operating in the EOT regime). The grating transmission as a function of incidence angle was also measured. A broadband mid-IR source was focused on the grating through a wire-grid polarizer passing only horizontally (x) polarized light, and transmission spectra were collected as a function of sample rotation around the vertical (y) axis. A clear splitting of the primary transmission peak is seen (Fig. 2(a)), corresponding to lifted degeneracy of the (1,0) and (-1,0) modes resulting from the non-zero in-plane incident photon momentum.

Control of the spectral properties of the EOT grating was achieved by thermal tuning. An increase in device temperature results in a linear shift ($n=3.255(1+4.5\times 10^{-5}\text{ T(K)})$ [28]) in the refractive index of the GaAs substrate, changing the resonant frequency of the plasmonic structure. The sample was affixed to a temperature-controlled transmission mount and GaAs band edge photoluminescence was used to calibrate a thermocouple at the base of the sample to the GaAs/metal interface temperature [21]. The achievable tuning range was measured by collecting transmission spectra as a function of sample temperature from $25\text{ }^\circ\text{C}$ to $235\text{ }^\circ\text{C}$. As shown in Fig. 2(b), the tuning of the grating results in a 20 cm^{-1} ($0.2\text{ }\mu\text{m}$) redshift of the transmission peak. Peak transmission of the grating decreased by $\sim 30\%$ (from 33% to 23%) as a result of the heating. We believe this decrease in transmission is due primarily to an increase in the metal losses at elevated temperatures, as the intrinsic carrier concentration of GaAs at 500K is not sufficient to result in significant free carrier losses in the substrate [29].

In order to demonstrate control of the coupling of light to propagating surface modes, a dual wavelength, liquid nitrogen-cooled, quantum cascade laser (QCL), operated pulsed at 80kHz with 100ns, 2.5A pulses, emitting at 1027 cm^{-1} ($\sim 9.7\text{ }\mu\text{m}$) and 1725 cm^{-1} ($\sim 5.8\text{ }\mu\text{m}$) (Fig. 1(a)), was used as the exciting source. The laser's long wavelength line is nearly resonant with the EOT grating's primary transmission peak, while the $5.8\text{ }\mu\text{m}$ peak is far from any plasmonic resonance.

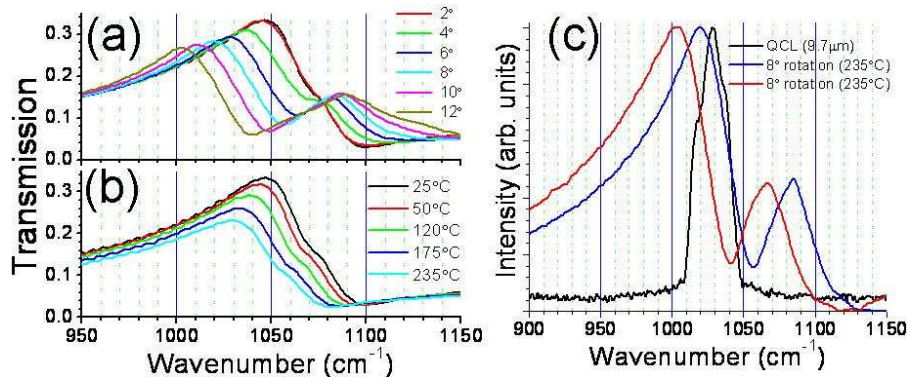


Fig. 2. (a) EOT grating transmission spectra as a function of incidence angle (RT) (b) Normal incidence EOT transmission for sample temperatures from RT to $235\text{ }^\circ\text{C}$ (c) Long wavelength QCL spectra and EOT transmission spectra at RT and $235\text{ }^\circ\text{C}$ for 8° angle of incidence.

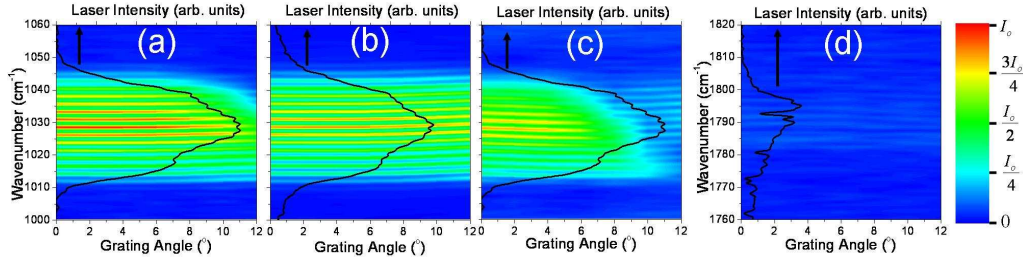


Fig. 3. Laser light transmitted through EOT grating as a function of wavenumber (cm^{-1}) and incidence angle for selected polarizations, laser lines, and sample temperatures (a) x-polarized, long wavelength (LW), RT (b) y-polarized, LW, RT (c) x-polarized, LW, 235°C (d) x-polarized, short wavelength, RT. The same color limits are used for each contour plot, with I_0 corresponding to the maximum transmitted laser intensity in (a). The overlaid spectra show the laser emission incident on the sample for each polarization and wavelength range plotted.

Transmission spectra for the dual wavelength QCL incident upon the EOT grating were obtained for incidence angles from 0-12° (rotation about the y-axis), grating temperatures from 25°C to 235°C, and for both x and y polarized light (as depicted in Fig. 1(d)). Representative transmission spectra are shown in Fig. 3. At room temperature (RT), the x-polarized 9.7 μm laser shows clear transmission to incident angles of 10° (Fig. 3(a)), but when the transmission spectrum of the EOT grating is redshifted, laser transmission cuts off at approximately 6° (Fig. 3(c)). No dramatic cut-off of transmission as a function of incidence angle is seen for y-polarized laser light (Fig. 3(b)), as a rotation around the y-axis only changes the in-plane incident photon momentum in the x-direction. The transmission of the 5.8 μm light is significantly weaker than that of the longer wavelength radiation and shows no dramatic effect in response to sample rotation (Fig. 3(d)). Because this laser line is spectrally distant from any grating transmission peak, it does not couple to any surface excitation. While this data demonstrates the ability to tune transmission of the EOT grating, it cannot provide any direct information on the coupling of the radiation to surface waves.

In order to image the propagation of the surface modes, a razor blade was attached to motorized translational stage, and aligned to travel across the metal side of the sample. At each step of the blade along the sample surface, the FTIR collects a separate spectrum $f_n(\nu)$, at the blade position x_n . Spectra from adjacent steps ($f_n(\nu)$, $f_{n+1}(\nu)$) are then subtracted and a difference spectra, $df_n(\nu)$, is generated and added to a difference spectra matrix. The difference spectra collected represent the differential amount of light blocked with each step of the blade, namely the light transmitted through the grating between blade positions x_n and x_{n+1} . The 9.7 μm laser light is focused onto the EOT surface to a spot size of $\sim 75 \mu\text{m}$ and transmitted/scattered light as a function of frequency and x-position is measured across the sample surface.

Control of SPP propagation on the surface should be achievable when a resonant frequency of the EOT grating can be tuned on and off the QCL laser line. Using the data from the angle-resolved broadband transmission tuning experiments, it was determined that an incidence angle of 8° would position the 9.7 μm QCL line on the (-1,0) room temperature EOT transmission peak. Upon tuning, this QCL line would move to sit on the high energy side of the peak, off of the transmission peak associated with the (-1,0) SPP mode (Fig. 2(c)).

At room temperature, when the long wavelength laser is spectrally aligned with the (-1,0) transmission peak, no propagation is seen on the sample surface, as evidenced by the isolated spot in Fig. 4(a). However, as the EOT grating is redshifted, the laser line now lies upon the high energy side of the (-1,0) peak and a distinct propagation of the incident light is seen, evidenced by the transmitted/scattered intensity tail extending in the -x direction from the laser spot. No propagation is detected for y-polarized light (though Fabry-Perot reflections at $x > 0$ are observed for both laser polarizations at all temperatures).

From the data in Fig. 4, we can estimate a decay length for the propagating excitation of approximately 384 μm . The calculated propagation length for a SPP [30], at this wavelength,

is $\sim 1000 \mu\text{m}$ for a Au/GaAs interface, using the complex dielectric Au found in Ref. [31]. This calculated propagation length is for a smooth Au-GaAs surface, though our sample uses a thin Ti adhesion layer and a periodically perforated metal. While scattering from the apertures no doubt shortens the propagation length of the excited surface waves, this scattering is also what allows for the visualization of the wave.

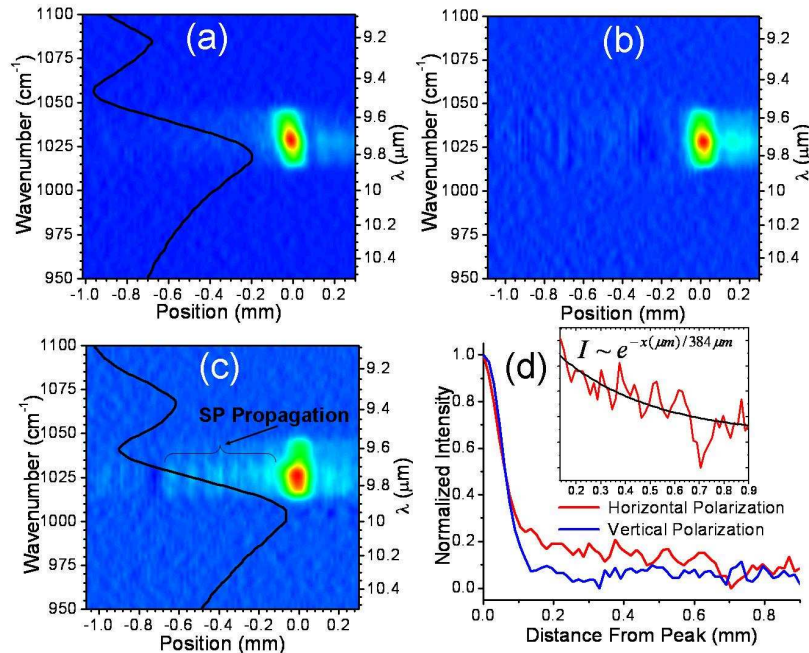


Fig. 4. Surface contour plots of transmitted light intensity as a function wavenumber (cm^{-1}) and x-position (mm) for (a) x-polarized light incident upon a RT grating (b) y-polarized and (c) x-polarized light incident upon a shifted (235°C) grating, with (c) showing the SP mode propagating in the $-x$ direction. The overlaid spectra in (a) and (c) show the EOT transmission at room and high temperature, respectively. (d) Intensity vs. position plot for $9.7 \mu\text{m}$ light incident upon the redshifted grating, with inset showing curve fit to decaying propagation tail. Fabry-Perot reflections for plots (a)-(c) can be seen on the $x > 0$ side of the laser spot.

The above results indicate that we are able to selectively excite propagating modes on the sample surface by active control of the EOT grating's optical properties. By studying the interaction of near-resonant QCL emission with a mid-IR EOT grating, we have demonstrated the distinct spectral positions of the EOT transmission maxima and the long range propagating surface modes on these mid-IR structures. In addition, this work demonstrates the feasibility of directional control of SPPs by use of a tunable plasmonic structure. While we have used thermal tuning to demonstrate this effect, tuning mechanisms utilizing voltage control of carrier concentrations at the semiconductor/metal interface hold the promise of much larger tuning ranges and significantly faster switching. For instance, in the current experiment, a device tuning range of $\sim 70 \text{ cm}^{-1}$ would allow the incident QCL light to switch between coupling to the $(-1,0)$ and $(1,0)$ modes, allowing for the design and fabrication of on-chip plasmonic routing devices and modulators. With more complex plasmonic structures, a full and continuous 360° of on-chip directional control may also be feasible.

Acknowledgments

The authors would like to thank L. Cheng and D. Bethke for laser overgrowth and sample fabrication assistance, respectively. Sandia is a multiprogram laboratory operated by Sandia Corporation, a Lockheed Martin Company, for the United States Department of Energy's National Nuclear Security Administration under contract DE-AC04-94AL85000.